ELSEVIER

Biochimica et Biophysica Acta 1323 (1997) 299–309

BIOCHIMICA ET BIOPHYSICA ACTA
BBA

Role of membrane lipid distribution in chlorpromazine-induced shape change of human erythrocytes

James Y. Chen, Wray H. Huestis *

Department of Chemistry, Stanford University, Stanford, CA 94305, USA

Received 21 February 1996; revised 6 August 1996; accepted 10 September 1996

Abstract

This is a study of the morphology and transbilayer lipid distribution of human erythrocytes treated with chlorpromazine (CPZ) over extended time courses. At 0°C, treatment of dilauroylphosphatidyl[1-^{14}C]choline-labeled erythrocytes with 120 μM CPZ produced an immediate stomatocytic transformation ($t_{1/2} < 5$ min) with no concurrent change in transbilayer distribution of radiolabeled lipid, as determined by bovine serum albumin extractability. At 37°C, CPZ treatment of cells produced two sequential morphological effects: immediate stomatocytosis ($t_{1/2} < 1$ min) with no concurrent change in radiolabel transbilayer distribution, followed by gradual increase in stomatocytic extent over several hours, with concurrent redistribution of radiolabeled lipid to the inner monolayer. Cells pretreated with vanadate at 37°C exhibited a triphasic morphological response: CPZ produced immediate stomatocytosis, followed by a transient reversion to echinocytes lasting about 2 h, before returning to stomatocytic morphologies over the next several hours. The echinocytic reversion was accompanied by exposure of phosphatidylserine on the cell surface, as indicated by increased activation of exogenous prothrombinase. These findings suggest that while CPZ induces transbilayer lipid redistribution over extended time periods (which may mediate the complex morphological transformations observed), the early stomatocytic response elicited by addition of CPZ is not due to lipid reorganization.

Keywords: Chlorpromazine; Vanadate; Erythrocyte shape change; Transbilayer lipid distribution; (Erythrocyte membrane)

1. Introduction

Chlorpromazine (CPZ) [1] is a phenothiazine drug used in treatment of schizophrenia. Its mode of action at the cellular level remains elusive; hence, much effort has aimed to characterize its interaction with various membrane systems. For example, CPZ-membrane interactions have been implicated in drug-induced effects on mitochondrial respiration [1] and sperm motility [2–4].

The human erythrocyte (rbc), having only one membrane and no internal organelles, is an ideal cell system for studying basic drug-biomembrane interactions. The lipids composing the erythrocyte membrane are distributed asymmetrically across the bilayer (see Refs. [5,6] for reviews). Choline-containing phospholipids, phosphatidylcholine (PC) and sphingomyelin (SM), are located mainly in the outer monolayer of the membrane, while aminophospho-

* Corresponding author. Fax: +1 (415) 7234817.

[1] Abbreviations: BSA: bovine serum albumin; CPZ: chlorpromazine; DLPC: dilauroylphosphatidylcholine; DLPS: dilauroylphosphatidylserine; dpm: disintegrations per minute; hct: hematocrit; MI: morphological index; PC: phosphatidylcholine; PS: phosphatidylserine; rbc: red blood cell.

PII S0005-2736(96)00197-6

lipids, phosphatidylserine (PS) and phosphatidylethanolamine (PE), are localized in the inner monolayer [7,8]. Lipid asymmetry control has been implicated in such physiological functions as removal of senescent erythrocytes from circulation [9–11] and hemostasis [12,13]. Lipid asymmetry is actively maintained by a vanadate-sensitive aminophospholipid translocase (flippase) that transports PS and PE from the outer to inner monolayer [14–16]. Recent studies have produced evidence that CPZ disrupts this asymmetry, inducing a transbilayer redistribution (scrambling) of membrane lipid [17,18].

However, the most pronounced membrane effect seen in CPZ-treated erythrocytes is a transformation from discoid to cupped morphology. To explain this change in shape, Sheetz and Singer [19] proposed a bilayer couple hypothesis, whereby amphipathic agents intercalating preferentially into the outer monolayer of the membrane bilayer would produce a net expansion of the outer monolayer, producing an outward buckling (echinocytosis or crenation), while amphipaths intercalating preferentially into the inner monolayer (such as CPZ) would produce an inward cupping or buckling (stomatocytosis). Demonstration that the net negatively-charged phospholipids are localized in the membrane inner monolayer [7,8] provided a physical rationale for the inner monolayer disposition of cationic amphipaths like CPZ, and direct evidence for this amphipath sequestration has been reported [20]. While inner monolayer intercalation provides a straightforward explanation for the observed shape change, membrane effects such as CPZ-induced lipid scrambling could play a role in the shape change mechanism [18]. In this study, the relationship between these two CPZ-induced effects was investigated further.

2. Materials and methods

2.1. Materials

Chlorpromazine hydrochloride, sodium orthovanadate, penicillin-streptomycin (lyophilized powder), 25% glutaraldehyde solution (grade I), bovine serum albumin (BSA, 96–99%), Triton X-100, and dilauroylphosphatidylethanolamine (DLPE) were obtained from Sigma Chemical Co. (St. Louis, MO). [^{14}C]Methyl iodide was obtained from Amersham Corporation (Arlington Heights, IL). Dilauroylphosphatidylserine (DLPS), A23187 ionophore, and prothrombin substrate (H-Sar-Pro-Arg-*p*NA, HCl) were obtained from Calbiochem (San Diego, CA). Factor V (bovine), Factor Xa (human), and prothrombin (human) were obtained from Enzyme Research Laboratories, Inc. (South Bend, IN). All other chemicals were reagent grade. Unless otherwise noted, reagents were used without further purification.

Dilauroylphosphatidyl[1-^{14}C]choline (^{14}C-DLPC) was synthesized based on previously published methods [21,22]. Lipid was purified on tapered silica gel G preparative thin-layer chromatography plates (Analtech, Inc., Newark, DE) in chloroform/methanol/formic acid (65:30:4, v/v). Final product was stored as a chloroform stock solution desiccated under argon at −20°C. Periodic assays of the stock solution by thin-layer chromatography showed no significant development of by-products or impurities.

2.2. Preparation of erythrocytes

Human blood was obtained from healthy volunteers by venipuncture, and collected in tubes containing citrate anticoagulant. Erythrocytes were washed 3 times by centrifugation ($1000 \times g$ for 5 min) in 150 mM NaCl, and the plasma and buffy coat were discarded. Isolated erythrocytes were then spun at $5000 \times g$ for 5 min, resuspended in 138 mM NaCl/5 mM KCl/7.5 mM sodium phosphate/1 mM $MgSO_4$/5 mM glucose (pH 7.4) (buffer A), and stored at 4°C until ready for use. Typically cells were used within 10 h of collection, and all cell incubations were done in capped plastic tubes. Final erythrocyte concentrations were 20% hematocrit (hct) unless otherwise noted.

2.3. Vesicle preparation

Stock lipid solutions were dried down under a gentle stream of argon or nitrogen, then resuspended in buffer A. Suspensions were bath-sonicated to clarity, to produce small unilamellar vesicles. In experiments employing PS, magnesium and glucose were omitted from buffer A and sonication was carried out under argon.

2.4. Incorporation of exogenous lipid into erythrocytes

For introduction of [^{14}C]DLPC, sonicated lipid vesicles were added to cells and the mixture was incubated at 37°C for 30 min. Cells were then washed by centrifugation and resuspension in buffer A to remove any unincorporated radiolabel. Final specific activity was 36 μCi l^{-1} packed cells (approx. 4 μM [^{14}C]DLPC in packed cells). For DLPS incorporation, erythrocytes were incubated with sonicated lipid vesicles for 90 min at 37°C (30–40 μM DLPS).

2.5. Treatment of erythrocytes with vanadate and chlorpromazine

Vanadate and CPZ were introduced to erythrocyte suspensions from stock solutions of phosphate-free isotonic saline (5 mM vanadate and 6 mM CPZ). Vanadate solutions were stored at room temperature, while CPZ solutions were prepared fresh daily. Typically vanadate stock solutions were prepared fresh monthly, although vanadate stock stored over 6 months appeared to inhibit PS translocation as completely as freshly made stock (data not shown).

Cell suspensions in buffer A were preincubated with 100 μM vanadate at 37°C for 10–20 min. Samples were then treated with 100–200 μM CPZ at 37°C for up to 8 h. At these CPZ concentrations, significant drug-membrane interactions are reported, with minimal cell lysis [17,19,20,23,24]. For incubations lasting 6 h or more, cell suspensions contained antibiotics (80 to 100 U penicillin/ml, 80 to 100 μg streptomycin/ml). For 0°C incubations, samples were transferred to a 0°C ice bath after vanadate preincubation, and allowed to sit at 0°C for 30 to 50 min before CPZ addition. In all experiments, control cell sample incubation times and temperatures were identical to incubations of experimental samples.

2.6. Treatment of erythrocytes with calcium

Calcium and ionophore were added to erythrocyte suspensions from stock solutions. Solutions of $CaCl_2 \cdot 2H_2O$ (5–50 mM) in phosphate-free isotonic saline were stored at 4°C; solutions of A23187 ionophore in ethanol/dimethyl sulfoxide (95:5, v/v) were stored at −20°C.

Cell samples in 135 mM KCl/5 mM NaCl/15 mM Hepes/1.2 mM $MgSO_4$/5 mM glucose (pH 7.4) (buffer B) were treated with 0.5 to 1.0 mM $CaCl_2 \cdot 2H_2O$ plus 5–10 μM A23187, at 37°C for 60 min. The high potassium content of buffer B prevents cell shrinkage due to calcium-activated K^+ efflux [25,26].

2.7. Morphology

Cell samples (less than 1% hct) were fixed with 0.3% glutaraldehyde in buffer A or B; this fixative concentration has been determined to provide adequate fixation with minimal pH effects [27,28]. Upon examination by light microscopy, individual cells were assigned a score based on shape [29–31]. Discocytes were assigned a score of 0; echinocytes were assigned scores from +1 (slightly echinocytic cells) to +5 (spheroechinocytes). Stomatocytes were assigned scores from −1 (monoinvaginated cells) to −4 (spherostomatocytes). The average score of a field of 100 cells was defined as the morphological index (MI) of that sample [30]. Typically, samples were counted twice, in random order, to obtain an average MI for each sample, and a standard deviation defined by the deviations of the two individual scores from the mean.

2.8. Extraction of [^{14}C]DLPC from erythrocytes with BSA (modified from [32])

Cell samples containing [^{14}C]DLPC were diluted to 5% hct in buffer A with or without BSA (10% w/v final concentration), and incubated at 37°C for 20 min. This treatment extracts radiolabeled lipids to a steady-state maximum; samples treated with BSA for an additional 25 min showed no additional extraction (data not shown). For vanadate-treated samples, all extraction buffers contained 100 μM vanadate. Following treatment with BSA, samples were pelleted by centrifugation at $13600 \times g$ for 30 s, and supernatants were removed. Pellets were lysed with Triton X-100 (8%, v/v), transferred to scintillation vials, and bleached by addition of sodium azide (20 mM) followed by hydrogen peroxide (6–9%, v/v). Sample vials were heated at 60–80°C overnight, then EcoLite scintillation cocktail (ICN Biomedicals, Inc., Irvine, CA) was added to each vial, and disintegrations per minute (dpm) for each pellet sample was

determined on a liquid scintillation counter, model LS 3801 (Beckman Instruments, Palo Alto, CA), using standard quench curves. Percentages of total radiolabel remaining in the pellets were calculated using the formula:

$$\%^{14}\mathrm{C} - \mathrm{PC\ in\ pellet} = 100 \times \frac{\mathrm{dpm\ from\ BSA} - \mathrm{extracted\ pellet}}{\mathrm{dpm\ from\ buffer\ A} - \mathrm{extracted\ pellet}} \quad (1)$$

2.9. Prothrombinase assay for outer monolayer PS (modified from [13,33,34])

Erythrocyte samples in buffer B were incubated at 37°C for 410 min, while treated concurrently with vanadate and CPZ, or calcium as described above, for time periods indicated in table legends. Samples then were washed 2–3 times by centrifugation at 1000–3000 × *g* for 5 min at 4°C, in 120 mM NaCl/50 mM Tris/6 mM $CaCl_2 \cdot 2H_2O$ (pH 7.8) (buffer C), ensuring removal of any membrane fragments. Following dilution to 0.1% hct with a mixture of factor V (5 nM), factor Xa (0.3 U ml^{-1}), and prothrombin (1.3 U ml^{-1}) in buffer C, samples were incubated at 37°C for 4–6 min to produce thrombin; this reaction was halted by the addition of 15 mM EDTA (pH 7.4). After centrifugation at 13600 × *g* for 30 s, supernatant aliquots were combined with 100 μM prothrombin substrate. Emergence of chromogenic cleavage product was monitored at 404 nm on a diode array spectrophotometer, model HP 8452A (Hewlett-Packard Co., Palo Alto, CA). Initial zero-order rates of absorbance increase (V_{max}) were determined using HP 89532 software (Hewlett-Packard Co.). Readings were not converted to actual concentrations of exposed PS, but were used to indicate the relative amounts of exposed PS in control and experimental samples.

2.10. Determination of hemoglobin

Results of the prothrombinase assay were normalized for hemoglobin concentration in each sample. For hemoglobin determination, cell samples were diluted 1:4 with 0.8 mM KCN/0.6 mM $K_3Fe(CN)_6$/1.0 mM KH_2PO_4 in Triton X-100 (0.05% v/v), allowed to react at room temperature for at least 30 min, and analyzed spectrophotometrically at 540 nm [35]. Supernatants of cell samples were also assayed in this manner to determine percent cell lysis per sample.

3. Results

All figures and tables report results of typical experiments.

3.1. CPZ-induced shape change in vanadate-treated erythrocytes

Cell suspensions were preincubated in buffer A in the presence or absence of vanadate, which inhibits active aminophospholipid translocation. Samples were then treated with CPZ and incubated at 0°C (Fig. 1A) or 37°C (Fig. 1B). Sample aliquots were removed at the indicated times and fixed for morphological analysis.

At 0°C (Fig. 1A), erythrocytes treated with 120 μM CPZ underwent a rapid ($t_{1/2} < 5$ min) discocyte-to-stomatocyte shape transformation that stabilized after approx. 1 h, when cells were predominantly monoinvaginated stomatocytes. This level of stomatocytosis was stable for at least 6 h at 0°C. Transformation of shape occurred whether or not cells were pretreated with 100 μM vanadate for 10 min, although typically slightly less stomatocytosis was observed with vanadate pretreatment. CPZ-free control cells remained discocytic over the 7 h incubation; vanadate-pretreated samples became slightly echinocytic.

At 37°C (Fig. 1B), samples treated with vanadate or CPZ alone exhibited shape transformations very similar to the same samples at 0°C; vanadate-treated cells crenated slightly, and CPZ-treated cells developed rapid stomatocytosis that was slightly greater than at 0°C. However, when CPZ was added to vanadate-pretreated cells at 37°C, a triphasic shape progression occurred, in contrast to stable stomatocytosis observed at 0°C. Cells at 37°C first underwent a stomatocytic transformation (from MI = −0.15 to −0.98) within the first minute of CPZ addition. With continued incubation, stomatocytosis was reversed, and by 70 min after CPZ addition, cells were slightly

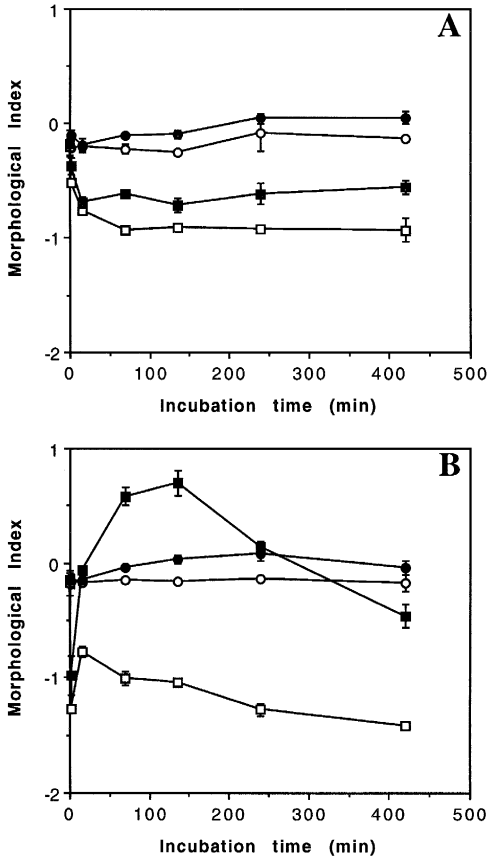

Fig. 1. Effect of vanadate pretreatment on CPZ-induced erythrocyte shape change at (A) 0°C or (B) 37°C. Cell samples were preincubated with (solid symbols) or without (open symbols) 100 μM vanadate for 10 min at 37°C. At time zero, cells were treated with (squares) or without (circles) 120 μM CPZ, then incubated at the indicated temperature. Aliquots were fixed for morphological analysis at the indicated times.

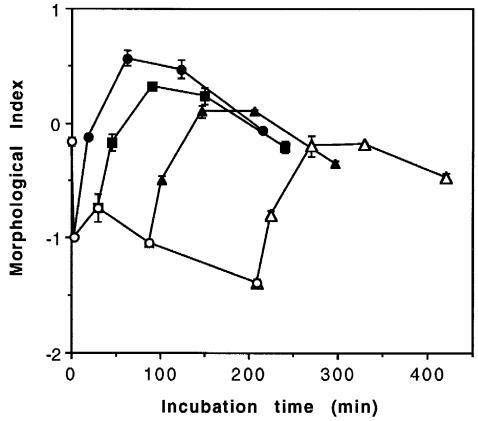

Fig. 2. Effect of vanadate posttreatment on CPZ-induced erythrocyte shape change at 37°C. At time zero, cell samples were treated with 120 μM CPZ (open circles). At the indicated times, sample aliquots were made 100 μM in vanadate, and incubated further at 37°C. The resulting morphologies were monitored (other symbols, as indicated).

echinocytic (MI = +0.58). Echinocytosis reached maximum extent by about 2 h, at which point a gradual stomatocytic reversion occurred, reaching MI = −0.46 by 7 h. Similar shape progressions were also induced when vanadate was added up to 3.5 h after CPZ addition (Fig. 2); in each case the stomatocytes reverted transiently toward echinocytic morphology, then returned again to cupped forms.

Table 1
Back-extraction of [^{14}C]DLPC with BSA, from CPZ-treated human erythrocytes at 0°C

CPZ concentration (μM)	Incubation time (min)	MI ± S.D. [a]	% dpm remaining in pellet after BSA extraction ± S.D.	% lysis
0	28	−0.01 ± 0.00	11.6 ± 0.9	0.6
	210	+0.05 ± 0.04	11.5 ± 0.7	n.d. [b]
	360	+0.08 ± 0.00	11.4 ± 0.5	2.5
120	13	−0.36 ± 0.02	11.6 ± 1.0	0.8
	100	−0.60 ± 0.06	11.5 ± 0.6	n.d.
	225	−0.74 ± 0.02	11.9 ± 0.9	1.6
	345	−0.81 ± 0.01	12.3 ± 0.7	2.4

Erythrocytes were treated with CPZ at 0°C for the specified incubation times, then extracted with BSA (10% w/v) at 37°C.
[a] S.D., standard deviation.
[b] n.d., not determined.

Table 2
Back-extraction of [^{14}C]DLPC with BSA, from CPZ-treated human erythrocytes at 37°C

CPZ concentration (μM)	Incubation time (min)	MI ± S.D. [a]	% dpm remaining in pellet after BSA extraction ± S.D.	% lysis
0	18	+0.03 ± 0.02	13.5 ± 1.2	0.6
	180	+0.05 ± 0.01	14.5 ± 0.6	n.d. [b]
	380	+0.02 ± 0.01	17.2 ± 1.0	2.0
120	3	−0.84 ± 0.01	13.0 ± 1.2	2.3
	95	−1.07 ± 0.01	19.0 ± 0.9	n.d.
	245	−1.25 ± 0.03	25.8 ± 1.2	3.1
	360	−1.26 ± 0.07	28.1 ± 1.1	3.6

Erythrocytes were treated with CPZ at 37°C for the specified incubation times, then extracted with BSA (10% w/v) at 37°C.
[a] S.D., standard deviation.
[b] n.d., not determined.

3.2. [^{14}C]DLPC back extraction of CPZ-treated erythrocytes

To assess the transbilayer distribution of PC in erythrocytes treated with CPZ at 0°C and 37°C, samples that had been prelabeled with [^{14}C]DLPC were subjected to extraction by BSA, to remove any radiolabeled lipid from the outer monolayer of the cells [18,36]. Radioactivity remaining with the cell pellet was attributed to radiolabeled lipid in the inner monolayer.

After short incubations, similar percentages of radiolabel dpm were retained in the pellets of CPZ-free samples at 0°C (11.6%) (Table 1), and at 37°C (13.5%) (Table 2), reflecting the normal predominant outer monolayer disposition of native PC [8]. At 0°C (Table 1), percentage of dpm inaccessible to BSA extraction changed very little over the course of a 6-h incubation in the presence or absence of CPZ. In CPZ-free cell samples, morphologies remained discoid throughout the incubation, while the percentage of pellet-associated dpm remained unchanged. Incubation with CPZ produced stomatocytosis to MI = −0.81 after 345 min, a change that was not accompanied by a significant increase in pellet-associated counts. This suggests that at 0°C, very little transbi-

Table 3
Effect of vanadate on extraction of [^{14}C]DLPC from CPZ-treated human erythrocytes (37°C)

Concentration (μM)		Incubation time (min)	MI ± S.D. [a]	% dpm remaining in pellet after BSA extraction ± S.D.	% lysis
Vanadate	CPZ				
0	0	115	−0.04 ± 0.02	11.9 ± 0.7	0.8
		435	−0.08 ± 0.06	13.8 ± 0.7	0.8
0	120	85	−0.96 ± 0.10	16.8 ± 1.0	n.d. [b]
		400	−1.44 ± 0.11	24.1 ± 1.1	2.3
100	0	135	+0.20 ± 0.01	12.6 ± 0.6	0.8
		450	−0.04 ± 0.01	16.4 ± 0.7	0.9
100	120	100	+0.80 ± 0.12	18.2 ± 1.3	2.5
		415	−0.91 ± 0.01	28.6 ± 1.0	2.6

Erythrocytes were pretreated with vanadate for 10 min at 37°C, treated with CPZ at 37°C for the specified incubation times, then extracted with BSA (10% w/v) at 37°C.
[a] S.D., standard deviation.
[b] n.d., not determined.

layer redistribution of PC occurred as cells became more stomatocytic.

At 37°C (Table 2), PC redistribution was apparent over time. Initially, there was no difference in relative radiolabel extractability between CPZ-free and CPZ-treated samples. In CPZ-free samples, pellet-associated dpm increased from 13.5% of total counts at 18 min to 17.2% at 380 min, while morphologies remained discoid. This suggests a slow redistribution of radiolabel from the outer to inner monolayer at 37°C over this time course, indicative of passive DLPC flip-flop [37,38]. With CPZ treatment, the fractional increase in pellet-associated dpm was much greater, rising from 13.0% of total counts after 3 min of CPZ treatment to 28.1% after 360 min of treatment. This indicates a drug-induced acceleration of PC transbilayer redistribution. Concurrently, cells became slightly more stomatocytic. However, CPZ-induced stomatocytosis had already developed at the earliest extraction time (MI = −0.84), while the shape change became only slightly more extensive with the following hours of incubation. Thus, as at 0°C, there is no apparent kinetic correlation between CPZ-induced PC scrambling and stomatocytosis.

Vanadate had no significant independent effect on the extractability of [^{14}C]DLPC at 37°C (Table 3). After 7.5 h of incubation, cells treated with 100 μM vanadate alone showed a slight increase in unextractable dpm compared to cells without vanadate, consistent with a previous report of vanadate-induced redistribution of PC in the bilayer [39]. Vanadate also did not have a significant effect on net radiolabel redistribution induced by CPZ. After 1.5–2.5 h of incubation at 37°C in the absence of vanadate, the unextractable PC fraction was 5% greater in the CPZ-treated sample than in the CPZ-free control (control, 11.9%; CPZ sample, 16.8%). A similar small increase was observed in samples pretreated with vanadate (control, 12.6%; CPZ sample, 18.2%). After 6.5–7.5 h of incubation, pellet-associated counts in each of the CPZ-treated samples had risen by 10–13% of the total, relative to the corresponding control (i.e., the fractional increase in pellet-associated counts was similar in the presence or absence of vanadate). These results are consistent with a similar study of vinblastine-invaginated cells, in which vanadate was not observed to affect the transbilayer distribution of spin-labeled sphingomyelin probes [18].

In all samples, percent cell lysis increased over time, but never exceeded 4% (Tables 1–3). However, since [^{14}C]DLPC extractability tended to decrease over time, this level of lysis did not compromise the qualitative interpretation of these results. Decreased accessibility of radiolabel with time was not due to BSA degradation; extended incubations of control samples enriched with 50% more [^{14}C]DLPC showed

Table 4
Prothrombinase assay for outer monolayer PS in vanadate/CPZ-treated erythrocytes at 37°C

Treatment	Incubation time +CPZ or Ca^{2+} (min)	MI ± S.D. [b]	AU/s ± S.D. (×10^3) [c]
100 μM vanadate [a]	0	−0.10 ± 0.01	2.94 ± 0.86
100 μM vanadate + 170 μM CPZ [a]	0	−1.22 ± 0.08	4.53 ± 0.04
	100	+0.08 ± 0.06	6.24 ± 1.03
	190	−0.22 ± 0.01	5.86 ± 0.03
	410	−1.17 ± 0.15	6.80 ± 0.29
900 μM Ca^{2+} + 6 μM A23187	65	+3.12 ± 0.16	19.58 ± 1.92

All erythrocyte samples were incubated at 37°C for 410 min. After 0, 220, 310, and 410 min, samples pre-equilibrated with vanadate were treated with CPZ, then incubated further. At t = 410 min, all samples were chilled and assayed for morphology and prothrombinase activity (normalized for hemoglobin concentration). A parallel control treated with vanadate only was incubated and assayed identically.
[a] Erythrocytes were preincubated with vanadate for 12 min prior to addition of CPZ.
[b] S.D., standard deviation.
[c] Initial zero-order increase in absorbance units per second (V_{max}) at 404 nm.

proportionately more extraction, indicating no significant decrease in the extraction capacity of BSA in this time domain (data not shown).

3.3. Prothrombinase assay for outer monolayer PS in vanadate-pretreated, CPZ-treated erythrocytes

To assess the transbilayer distribution of endogenous PS in erythrocytes, a prothrombinase assay was used. In this assay, the presence of outer monolayer PS initiates a coagulation cascade, resulting in a dose-dependent liberation of chromophore from prothrombin substrate [13,33,40]. This PS assay was chosen over others for two reasons. First, it assays for endogenous PS, eliminating the need for introducing foreign PS probes (such as short-chain PS homologs or spin labels) which may not necessarily mimic the behavior of the native species. In addition, the assay should not remove or destroy membrane components, thereby reducing disruptions in membrane activity and integrity [33].

Of the samples tested for outer monolayer PS (Table 4), cells treated with calcium and ionophore produced the highest rate of absorbance increase at 404 nm, indicating the most thrombin-induced cleavage of chromogenic substrate, and the most outer monolayer PS. This indicates extensive scrambling of membrane PS by calcium treatment, in agreement with previous reports [34,39,40]. Vanadate-treated cells without CPZ showed the lowest activity of the samples tested, producing only 15% of the activity seen with calcium-treated cells [2].

With the addition of CPZ to vanadate-pretreated cells at 37°C, prothrombinase activity increased with longer CPZ incubation times. Increase was apparent even after 410 min, when activity was 50% higher than in the sample initially exposed to CPZ (but still only 35% of the activity in the calcium-treated sample). This suggests a continual CPZ-induced movement of membrane PS from the inner to outer monolayer. Cell morphologies during this time course were typical of the triphasic shape progression seen with CPZ-treated cells pretreated with vanadate: stomatocytic upon CPZ addition (MI = −1.22), discocytic at 100 min (MI = +0.08), then gradually reverting to stomatocytes (MI = −1.17 at 410 min). Thus, there is no direct correlation between PS transbilayer distribution and the triphasic shape progression of these cells (Table 4).

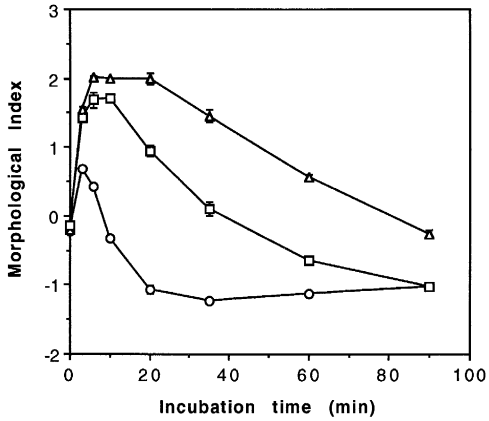

Fig. 3. DLPS-induced shape change of vanadate-pretreated erythrocytes at 37°C. Cells were preincubated with 100 μM vanadate for 0 min (circles), 15 min (triangles), or 7.5 h (squares). At time zero, 40 μM DLPS was added to each cell sample, and the resulting morphologies were monitored over time.

3.4. DLPS-induced shape change in vanadate-pretreated erythrocytes

The role of aminophospholipid translocation in long-term cell shape transformations was examined in vanadate-treated cells. Erythrocytes were preincubated at 37°C with vanadate for 7.5 h, the time required for vanadate-pretreated, CPZ-treated cells to pass through their triphasic shape change (Fig. 1B). Upon DLPS addition (Fig. 3), vanadate-free cells became slightly echinocytic after 3 min, followed by a stomatocytic transformation that stabilized by 20 min after lipid addition. Such a shape progression is indicative of exogenous PS incorporation into the outer monolayer to produce echinocytes, followed by conversion to stomatocytes as PS is transported to the inner monolayer [16].

With a 15-min vanadate preincubation followed by DLPS treatment (Fig. 3), cells became highly echinocytic (MI = +2.02 after 6 min), and did not

[2] When normalized for lipid phosphate, sonicated rbc membrane fragments produced a prothrombinase activation rate two-fold higher than cells calcium-loaded under the conditions noted. This result is offered for qualitative comparison; however, it is probably not valid to make quantitative comparisons of prothrombinase activation data obtained using membranes of widely varying configurations (M.S. Moxness, personal communication).

revert in shape until after 20 min of lipid incubation, eventually dropping to MI = −0.27 after 90 min of incubation with DLPS. With a 7.5-h vanadate preincubation, cells then treated with DLPS became similarly echinocytic (MI = +1.68 after 6 min). However, after only 10 min the shapes of these cells began to revert, returning to the morphology of vanadate-free cells after 90 min (MI = −1.03). These results indicate that with extended vanadate incubation, aminophospholipid translocase activity was partially restored.

4. Discussion

The mechanism of CPZ-induced stomatocytosis in erythrocytes has long been under study. Early work suggested [19] that stomatocytosis occurred by intercalation of cationic CPZ molecules into the anionic inner monolayer of the erythrocyte membrane, resulting in net inner monolayer expansion and inward membrane buckling (the bilayer couple hypothesis). Indeed, with a ghost membrane:aqueous phase partition coefficient of 1000 to 5500 [23,41,42], CPZ should readily incorporate into erythrocyte membranes. Recent studies suggest CPZ-induced effects involving cytofacial components such as skeletal proteins [43] and phosphoinositides [44], reinforcing the likelihood of an inner monolayer disposition.

Other studies implicate stomatocytic mechanisms more complicated than inner monolayer intercalation, such as inhibition of calmodulin-regulated activities [45] and CPZ-induced lipid scrambling [18]. However, CPZ-induced stomatocytosis does not appear to be related to either of these events. In the case of calmodulin inhibition, a number of stomatogenic amphipaths were found to inhibit calmodulin very little [46]. CPZ-induced shape change was also not correlated with changes in calmodulin-dependent membrane protein phosphorylation [47]. Additionally, metabolic processes (such as those regulated by calmodulin and calmodulin-dependent kinases) are inhibited significantly at low temperatures. If calmodulin inhibition were solely responsible for stomatocytosis, then cooling normal cells to 0°C should produce a stomatocytic response. In fact, normal cells remain discoid upon cooling to 0°C (Fig. 1A).

The lipid scrambling mechanism provides an alternative based not on the bilayer distribution of CPZ, but on redistribution of endogenous lipids. Schrier and co-workers [18] propose that CPZ and related amphipaths may induce stomatocytosis by a combination of (1) drug-induced bilayer scrambling of all phospholipids, which could introduce aminophospholipids to the outer monolayer without affecting morphology; and (2) flippase-mediated selective translocation of aminophospholipids back to the inner monolayer. Absent a rapid mechanism for restoring scrambled choline lipids to the outer monolayer, these events result in net expansion of the inner monolayer. Several of the present findings are inconsistent with this hypothesis as the primary mode of CPZ action. First, the model invokes two temperature-sensitive processes, phospholipid flip-flop and aminophospholipid translocation, both of which are inhibited severely at 0°C. If the immediate cause of CPZ-induced stomatocytosis is translocation of scrambled PS, then no CPZ effect should be apparent at 0°C. In fact, CPZ induces rapid ($t_{1/2} < 5$ min) stomatocytosis at 0°C, under conditions where PS transport is abolished [48]. BSA extraction of [^{14}C]DLPC indicates that CPZ-induced lipid scrambling is likewise inhibited at 0°C (Table 1). While the magnitude of CPZ stomatocytosis is greater at 37°C than at 0°C (Fig. 1), its occurrence at 0°C cannot be attributed to phospholipid redistribution.

The CPZ-induced shape effect can also be decoupled from lipid scrambling at 37°C, by using a concentration of CPZ that generates only monoinvaginated stomatocytes and by analyzing very early cell responses (Table 2). Although both CPZ-induced redistribution of [^{14}C]DLPC and gradual increase in stomatocytic extent are observed over time, consistent with native PC scrambling, substantial stomatocytosis is evident well before [^{14}C]DLPC redistribution can be detected. Thus, lipid scrambling does not appear to play a role in the immediate drug-induced shape change at 37°C, but may be important in mediating subsequent morphological events. The earlier study [18] employed higher drug concentrations than this work, which may accelerate the phospholipid redistribution. This would complicate interpretation by superimposing several complex but kinetically distinguishable responses.

The lipid redistribution mechanism is also not supported by results of experiments using vanadate-

pretreated erythrocytes. Earlier reports provide evidence that drug-induced stomatocytosis and endocytosis are inhibited in the presence of vanadate [18,49]. Indeed, immediately upon addition of vanadate to CPZ-treated cells, stomatocytosis begins to reverse (Fig. 2), consistent with those reports. Such inhibition could reflect outer monolayer expansion by drug-scrambled aminophospholipid, trapped in the outer monolayer due to flippase inactivation [18]. However, if cells are pretreated with vanadate and then exposed to low concentrations of CPZ, an early immediate stomatocytosis is observed, followed by reversion to echinocytes over a 1-h interval (Fig. 1B). Unless early time-points are monitored, the overall shape effect appears to be simple inhibition of stomatocytosis. Thus, as with vanadate-free cells, the biphasic nature of the shape change seen with vanadate pretreatment suggests a two-event process: intercalation of CPZ to produce immediate stomatocytosis, followed by general drug-induced lipid scrambling (Table 3) and net redistribution of PS to the outer monolayer resulting in crenation. Such accumulation of PS in the outer monolayer is indicated by the increased prothrombinase activity of these cells with time (Table 4).

Prolonged incubations of cells with vanadate and CPZ reveal a third phase in this complex shape response: a gradual reversion to stomatocytes over several hours. The mechanism behind this phase of the shape change is not evident, as several aspects are difficult to reconcile with any simple model. During the time frame of the third shape response, vanadate inhibition of the flippase is apparently partially reversed, as indicated by morphology assay (Fig. 3). This might suggest that several hours after vanadate and CPZ addition, flippase activity is partially restored, allowing scrambled outer monolayer PS to be slowly transported back into the inner monolayer, producing stomatocytes [3]. However, in this same extended time domain, activation of prothrombinase increases slightly (Table 4), which is not consistent with a net inward movement of PS. Hence, the mechanism behind this part of the triphasic shape change appears to be complex, and requires further study.

While lipid scrambling may offer a partial contribution to overall CPZ-induced stomatocytosis, it appears that selective inner monolayer intercalation of the amphipath still provides the most general explanation for its morphological effects. Ongoing studies will address preferential binding of CPZ with cytofacial membrane components.

[3] CPZ is reported to reduce vanadate to vanadyl cation in free aqueous solution [50], and intracellular vanadyl acts as a relatively inefficient flippase inhibitor [51].

Acknowledgements

The authors wish to thank Dr. Linda Brunauer for her involvement with the radioactive lipid synthesis and the prothrombinase assay, and Dr. Margaret Maulucci-Gedde for her input during the initial stages of the 0°C studies. This work was supported by USPHS grant R01 HL 23787.

References

[1] Matsubara, T. and Hagihara, B. (1968) J. Biochem. 63, 156–164.
[2] Cates, N.R. and Jozefowicz, T.H. (1970) Res. Commun. Chem. Pathol. Pharmacol. 1, 223–229.
[3] Peterson, R.N. and Freund, M. (1975) Biol. Reprod. 13, 552–556.
[4] Hong, C.Y., Chaput de Saintonge, D.M. and Turner, P. (1982) Eur. J. Clin. Pharmacol. 22, 413–416.
[5] Devaux, P.F. (1991) Biochemistry 30, 1163–1173.
[6] Schroit, A.J. and Zwaal, R.F.A. (1991) Biochim. Biophys. Acta 1071, 313–329.
[7] Bretscher, M.S. (1972) Nature (London) New Biol. 236, 11–12.
[8] Verkleij, A.J., Zwaal, R.F.A., Roelofsen, B., Comfurius, P., Kastelijn, D. and Van Deenen, L.L.M. (1973) Biochim. Biophys. Acta 323, 178–193.
[9] Schlegel, R.A., McEvoy, L. and Williamson, P. (1985) in Bibliotheca Haematologica (Hässig, A., ed.), Vol. 51, pp. 150–156, Karger, Basel.
[10] McEvoy, L., Williamson, P. and Schlegel, R.A. (1986) Proc. Natl. Acad. Sci. USA 83, 3311–3315.
[11] Schwartz, R.S., Tanaka, Y., Fidler, I.J., Chiu, D.T., Lubin, B. and Schroit, A.J. (1985) J. Clin. Invest. 75, 1965–1972.
[12] Bevers, E.M., Comfurius, P., Van Rijn, J.L.M.L., Hemker, H.C. and Zwaal, R.F.A. (1982) Eur. J. Biochem. 122, 429–436.
[13] Bevers, E.M., Comfurius, P. and Zwaal, R.F.A. (1983) Biochim. Biophys. Acta 736, 57–66.
[14] Bitbol, M., Fellmann, P., Zachowski, A. and Devaux, P.F. (1987) Biochim. Biophys. Acta 904, 268–282.

[15] Seigneuret, M. and Devaux, P.F. (1984) Proc. Natl. Acad. Sci. USA 81, 3751–3755.
[16] Daleke, D.L. and Huestis, W.H. (1985) Biochemistry 24, 5406–5416.
[17] Rosso, J., Zachowski, A. and Devaux, P.F. (1988) Biochim. Biophys. Acta 942, 271–279.
[18] Schrier, S.L., Zachowski, A. and Devaux, P.F. (1992) Blood 79, 782–786.
[19] Sheetz, M.P. and Singer, S.J. (1974) Proc. Natl. Acad. Sci. USA 71, 4457–4461.
[20] Elferink, J.G.R. (1977) Biochem. Pharmacol. 26, 2411–2416.
[21] Stockton, G.W., Polnaszek, C.F., Leitch, L.C., Tulloch, A.P. and Smith, I.C.P. (1974) Biochem. Biophys. Res. Commun. 60, 844–850.
[22] Ferrell, J.E., Lee, K. and Huestis, W.H. (1985) Biochemistry 24, 2849–2857.
[23] Lieber, M.R., Lange, Y., Weinstein, R.S. and Steck, T.L. (1984) J. Biol. Chem. 259, 9225–9234.
[24] Olivier, J.L., Chachaty, C., Wolf, C., Daveloose, D. and Bereziat, G. (1989) Biochem. J. 264, 633–641.
[25] Sarkadi, B., Szász, I. and Gárdos, G. (1976) J. Membr. Biol. 26, 357–370.
[26] Ferrell, J.E. and Huestis, W.H. (1982) Biochim. Biophys. Acta 687, 321–328.
[27] Morel, F.M.M., Baker, R.F. and Wayland, H. (1971) J. Cell Biol. 48, 91–100.
[28] Gedde, M.M. (1993) Ph.D. thesis, Stanford University.
[29] Bessis, M. (1973) in Red Cell Shape: Physiology, Pathology, Ultrastructure (Bessis, M., Weed, R.I. and Leblond, P.F., eds.), pp. 1–25, Springer-Verlag, New York.
[30] Fujii, T., Sato, T., Tamura, A., Wakatsuki, M. and Kanaho, Y. (1979) Biochem. Pharmacol. 28, 613–620.
[31] Daleke, D.L. and Huestis, W.H. (1989) J. Cell Biol. 108, 1375–1385.
[32] Lin, S., Yang, E. and Huestis, W.H. (1994) Biochemistry 33, 7337–7344.
[33] Connor, J., Bucana, C., Fidler, I.J. and Schroit, A.J. (1989) Proc. Natl. Acad. Sci. USA 86, 3184–3188.
[34] Brunauer, L.S., Moxness, M.S. and Huestis, W.H. (1994) Biochemistry 33, 4527–4532.
[35] Van Kampen, E.J. and Zijlstra, W.G. (1961) Clin. Chim. Acta 6, 538–544.
[36] Mohandas, N., Wyatt, J., Mel, S.F., Rossi, M.E. and Shohet, S.B. (1982) J. Biol. Chem. 257, 6537–6543.
[37] Fujii, T. and Tamura, A. (1983) Biomed. Biochim. Acta 42, S81–S85.
[38] Loh, R.K. and Huestis, W.H. (1993) Biochemistry 32, 11722–11726.
[39] Williamson, P., Kulick, A., Zachowski, A., Schlegel, R.A. and Devaux, P.F. (1992) Biochemistry 31, 6355–6360.
[40] Comfurius, P., Senden, J.M.G., Tilly, R.H.J., Schroit, A.J., Bevers, E.M. and Zwaal, R.F.A. (1990) Biochim. Biophys. Acta 1026, 153–160.
[41] Roth, S. and Seeman, P. (1972) Biochim. Biophys. Acta 255, 207–219.
[42] Luxnat, M. and Galla, H. (1986) Biochim. Biophys. Acta 856, 274–282.
[43] Minetti, M. and Di Stasi, A.M.M. (1987) Biochemistry 26, 8133–8137.
[44] Bütikofer, P., Lin, Z.W., Kuypers, F.A., Scott, M.D., Xu, C., Wagner, G.M., Chiu, D.T. and Lubin, B. (1989) Blood 73, 1699–1704.
[45] Nelson, G.A., Andrews, M.L. and Karnovsky, M.J. (1983) J. Cell Biol. 96, 730–735.
[46] Isomaa, B. and Engblom, A.C. (1988) Biochim. Biophys. Acta 940, 121–126.
[47] Reinhart, W.H., Sung, L.A., Schuessler, G.B. and Chien, S. (1986) Biochim. Biophys. Acta 862, 1–7.
[48] Daleke, D.L. (1986) Ph.D. thesis, Stanford University.
[49] Schrier, S.L., Junga, I. and Ma, L. (1986) Blood 68, 1008–1014.
[50] Vyskocil, F., Pilar, J., Zemkova, H. and Teisinger, J. (1982) Lancet 1, 1078–1079.
[51] Loh, R.K.H. (1988) M.S. thesis, Stanford University.